

Optimization of Laser Micro/Nano Processing of Silicon and Quartz

Muaath J. Mahmoud^{a,*}, Bassam G. Rasheed^b and Muammel M. Hanon^c

^aLaser Research Center, Directorate of Materials Research, Ministry of Science and Technology, Baghdad 10070, Iraq.

^bLaser & Optoelectronics Engineering Department, College of Engineering, Al-Nahrain University, Baghdad 10072, Iraq.

^cBaquba Technical Institute, Middle Technical University, Baghdad 10074, Iraq.

*Corresponding author. Tel.: +964-770-780-8074; e-mail: muaathjamal@yahoo.com

ABSTRACT

This research paper explores the application of three laser systems, namely the Nd:YAG laser, fiber laser, and CO₂ laser, for the micro/nano machining of silicon and quartz materials. The experimental results demonstrate the successful formation of stable silicon nanoparticles with reduced dimensions. Additionally, a quartz sheet was utilized to create a microlens array. The laser microprocessing technique was enhanced through the implementation of design of experiments (DOE) analysis. A Box-Behnken design (BBD) software was employed to conduct 17 tests, investigating the influence of laser parameters on the microprocessing outcomes. The COMSOL software was utilized for theoretical calculations to determine the distribution of surface temperatures and subsurface temperatures of silicon and quartz. The maximum temperatures achieved were approximately 5700 K for silicon and 2630 K for quartz. Numerical optimization using DOE software improved the production of silicon nanoparticles and quartz microlens, producing silicon nanoparticles wavelength peak and absorption peak values of 318.2 nm and 0.39, respectively. Additionally, quartz microlens numerical aperture and surface roughness improved to 0.494 and 4.64 nm, respectively. Due to the precise control offered by the laser micro/nano machining process, the findings of this study hold potential for diverse applications in optoelectronics and biological imaging that can leverage the unique characteristics of silicon nanoparticles and microlens arrays.

Keywords: laser micro/nano processing, silicon nanoparticles, microlens array, design of experiments.

1. INTRODUCTION

Laser microprocessing of brittle materials has attracted great efforts for decades, such as silicon and glass. This critical technology is for manufacturing precision parts and components used in a wide range of industries, including electronics, optoelectronics, and aerospace applications [1].

The laser ablation involves the rejection of material due to the generation of high vapor pressure. Laser ablation of solid targets in liquids (LAL) is an excellent way to make nanoparticles because it is easy to control, quick, and good for the environment. It protects against the risk of contamination for the silicon nanoparticles (NPs) made in a big way [5].

Silicon has been the subject of extensive study. It is a typical substrate material for many different types of electronic devices and finds comprehensive application in the semiconductor sector. In both solar cells and other types of chips, polycrystalline and amorphous silicon can be used [8].

Moreover, glass can be used for many different micro and nanotechnology tasks. The inertness and other thermomechanical properties of glass are also very appealing [9]. Glass machining is getting a lot of attention these days because glass microstructures are used in fields like biomedicine, biochemistry, lab-on-a-chip devices, sensors, and hydrophobic applications [10].

Sherpa and Pradhan [10] performed micro-grooving of a silicon wafer using Nd:YAG laser with 20 μm diameter, 8 μJ. The groove diameter was 508 μm. The research showed that when increasing the laser frequency; the surface roughness increased. Schmidt and Conrad [11] made the MLA for glass using a 200 ns pulse CO₂ laser with a galvanometer ablation and as and 700 W CW CO₂ laser for polishing. The size of microlens was 300–500 μm. The manufacturing procedure is adaptable, highly reproducible, and quick. Al-Kattan et al. [12] synthesized silicon nanoparticles using a femtosecond (Fs) laser in 2 steps. First, applying laser ablation, which is laser directed to the silicon wafer in DW. The final step is applying the fragmentation process. The Fs laser has wavelengths 1025 nm, 480 fs pulse duration, and 1 KHz PRR. The silicon NPs were used in photodynamic therapy on breast cancer. The research shows that Si nanoparticles the fragmentation process reduced Si NPs from 92 nm to 62 nm. Wang et al. [13] fabricated concave silicon MLA using Fs laser and dry etching. The Fs with 343 nm wavelength, 280 fs pulse duration, and 200 KHz PRR was used to remove the material. The mixed gases were applied to reduce the surface roughness. The fabricated ML has a 7-9 μm focal length with a roughness was 5.56 nm. The research showed when increasing the laser power, the reduction of curvature decreased, and the diameter increased. Moreover, the orientation of silicon crystals does not have a significant effect on the fabrication process.

This research explores the optimization of laser micro/nano processing of silicon and quartz, employing three different lasers, and utilizes design of expert analysis (DOE) to enhance the laser microprocessing technique. The study investigates the formation of tiny, stable silicon nanoparticles and the creation of a quartz microlens array, contributing to the field of laser ablation and nanotechnology applications. The experimental and theoretical investigation provides insights into the optimization process for synthesizing silicon nanoparticles and producing quartz microlenses, offering potential advancements in optoelectronics, biological imaging, and precision manufacturing.

2. EXPERIMENTAL METHODS

Before the experimental fabrication process, the theoretical calculations were made using Mathcad software (15) to calculate the surface temperature of silicon and quartz material to determine the laser parameters of material processing.

A 1064 nm Nd:YAG laser with the following specifications: pulse duration of 10 ns, spot size, was 1 mm, output energy 20-2000 mJ, and pulse repetition rate (PPR) of 1-10Hz, was applied on a silicon wafer of 500 μm thickness.

While fiber laser of 1064 nm with the following specifications: output power 1-30 W, power density was 0.2-6 *10⁵ W/cm², spot size of 0.1 mm, laser speed of 1-1000 mm/s and CO₂ laser of 10.06 μm with the following specifications: output power 1-100 W, spot size of 1 mm, laser speed 1-6 mm/s were applied to a quartz sheet of 1.1 μm thickness.

The PLAL process was used to synthesize silicon nanoparticles in water. The silicon wafer was placed in a plastic container, fulfilled with 2.5 ml of distilled water (DW), and subjected to 300 laser pulses. Then, the suspension was also subjected to fiber laser for 10 minutes to obtain silicon nanoparticle suspension, this process is known as "fragmentation".

On the other side, production of quartz microlenses is a two-step process. First, fiber laser with a galvo system was applied to the sheet's surface to remove the material using specific laser parameters. The second step involves

reshaping the surface of the quartz sheet using a CO₂ laser beam; this is known as "resurfacing".

Before any processing could begin, an ultrasonic device was used to wash the silicon wafer and quartz sheet with ethanol and distilled water.

High-resolution optical microscope OLYMPUS BX60M was used to examine the silicon wafer and quartz sheet to see where they had interacted. The optical microscope images were saved, and (ImageJ) software was used to measure the dimensions of the manufactured microlens.

Furthermore, an optical absorption spectrometer (Model Metrech SP8001) was employed to collect data in the wavelength range of 300–700 nm. Finally, using DOE software to analyze the results statistically, then make the optimization process.

3. RESULTS AND DISCUSSION

Extensive experimental investigation and theoretical calculations were performed on the constructed microlenses and silicon nanoparticles.

3.1 Theoretical Calculations

The laser's energy is absorbed by the surface of the silicon and quartz target, leading to heating, melting, and vaporization [14].The melting and vaporization temperatures for silicon were 1687 K and 3538 K, respectively. At the same time, the melting and vaporization points for quartz were measured to be 1923 K and 2503 K, respectively [10]. The high energy density of the laser causes a rapid rise in temperature at the surface of the silicon and quartz after a short time of exposure to the laser beam. It is possible to determine the surface temperature using the relation (1)[15]:

$$T = \alpha F A / (p c_p) \tag{1}$$

In this equation, the absorption coefficient (α), the energy density (F), the absorptivity (A), the density (p) and the specific heat (c_p). Table 1 gives the surface temperature for silicon and quartz as a function with the laser energy/power.

Table 1 Silicon and quartz surface temperature as a function of laser energy and power respectively

Nd:YAG laser		Fiber laser		CO ₂ laser	
E(J)	Silicon Temp.(K)	P(W)	Quartz Temp. (K)	P(W)	Quartz Temp. (K)
0.2	1137	4	760	2	825
0.4	2275	7	1320	4	1650
0.6	3411	13	2480	6	2480
0.8	4548	19	3590	8	3300
1	5685	22	4150	10	4130

The theoretical model of the laser's interaction with the silicon and quartz was developed using the COMSOL

software. Figure 1 shows how the model simulates the surface heat for silicon and quartz.

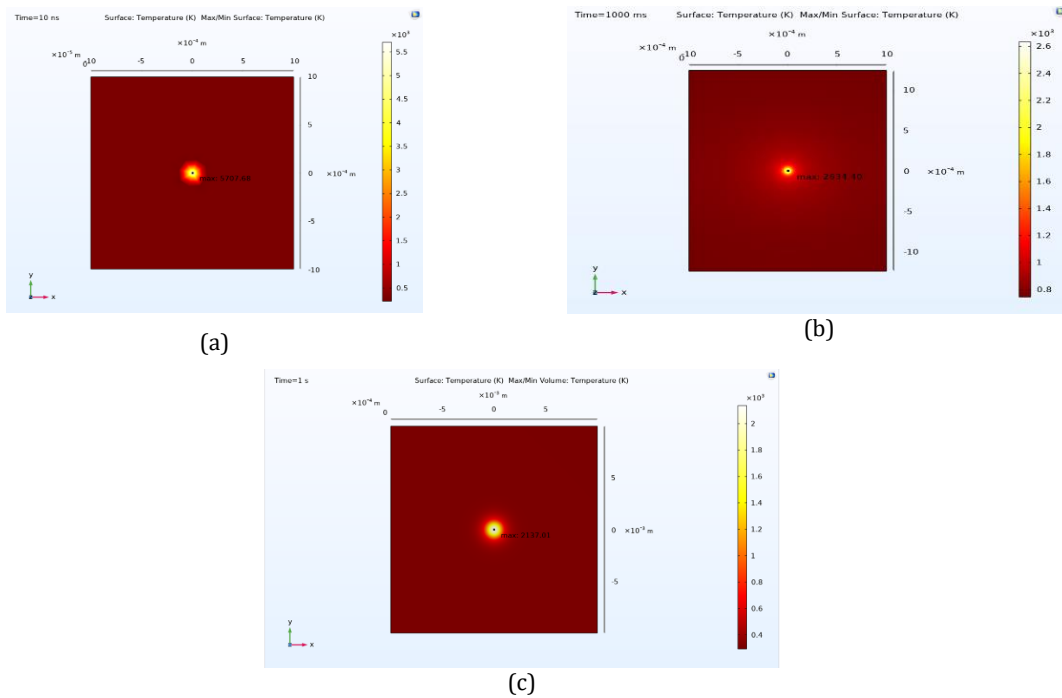


Figure 1. The theoretical model of silicon and quartz irradiated by Nd:YAG laser , fiber laser and CO₂ laser respectively. (a) max temperature at the surface of silicon by Nd:YAG laser (b) max temperature at the surface of quartz by fiber laser (c) max temperature at the surface of quartz by CO₂ laser.

The temperature of silicon and quartz at various times for different lasers is shown in Figure 1. As demonstrated in Figure 1, silicon surface temperature is about 5700 K. In contrast, quartz surface temperature is approximately 2630 K for fiber laser and 2140 K for CO₂ laser as shown in

Figure 1(a, b, c) respectively. Furthermore, when the lasers are irradiative the silicon and quartz substrate, immediately heated up and the processing starts, as shown in Figure 2.

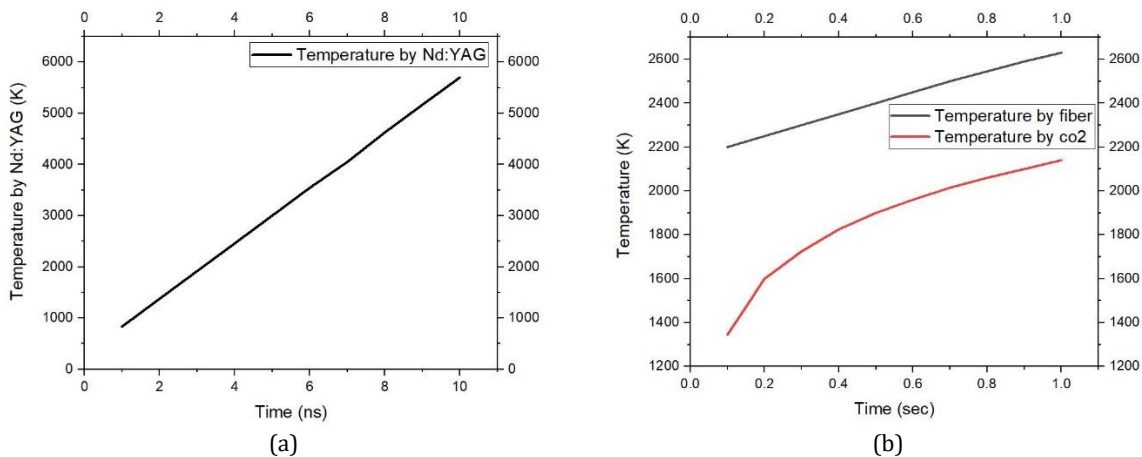


Figure 2. The surface temperature of : (a)silicon by Nd:YAG laser (b) quartz by fiber and CO₂ laser.

Due to silicon's strong absorption rates at 1064 nm, it requires low energy with a short time to achieve the ablation process. In contrast, quartz has a low absorption rate of 1064 nm, which requires high power and a long time to achieve the ablation process. Unlike the CO₂ laser/quartz interaction, the laser power is sufficient to heat up the quartz due to strong absorption for 10.6 μm [16].

3.2 The Irradiation Area

The irradiation area of silicon wafer with Nd:YAG laser and the quartz sheet with fiber laser followed by CO₂ laser are shown in Figure 3. It has been discovered that the form of the interaction area on the silicon surface is quite close to being spherical. As can be seen in Figure 3(a), the diameter of the interaction area measures 800 μm. Although it has

spherical morphologies, the interaction area of quartz has a diameter of 200 μm, as shown in Figure 3(b).

The difference in the diameter between each shape is due to the difference in the spot size of each laser, which is 2 mm for the Nd:YAG laser and 0.1 mm for the fiber laser.

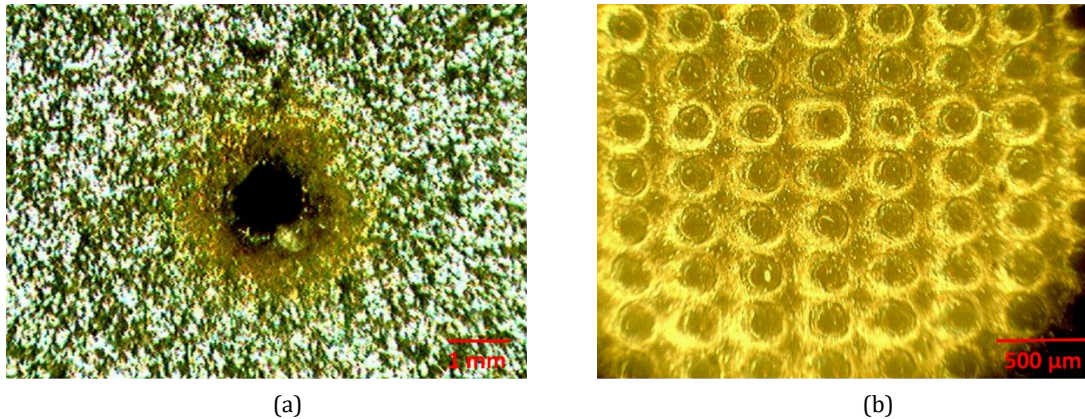


Figure 3. The optical microscope image of the interaction area of (a) silicon and (b) quartz.

3.3 Statistical Analysis and Numerical Optimization

Design-Expert is a software package developed by Stat-Ease Inc. that is specifically designed to conduct design of experiments (DOE) in a statistical context. Design Expert provides a range of analytical methodologies, including comparison tests, screening, characterization, optimization, resilient parameter design, mixture designs, and combined designs. The (BBD) was used to study the impact of three input variables [17]. Nd:YAG laser energy, pulse number and PPR on a silicon wafer of a thickness of 500 μm.

Furthermore, to evaluate effects of three fiber laser inputs, laser power, exposure time, and speed on a 1.1 mm thick quartz sheet. Several process parameters were selected in an experimental setting based on the laser source's ability to modify these parameters.

An ANOVA examined responses (output parameters) impacted by numerous variables (input parameters). Each experiment changed input factors to determine response variables. To build a mathematical model with the fewest mistakes that linked inputs and outputs (parameters and responses). A generic quadratic equation was used to predict the reaction for different element quantities, as demonstrated by [18]:

$$y = \beta_0 + \sum_{i=1}^m \beta_i x_i + \sum_{i=1}^m \beta_{ii} x_i^2 + \sum_i \sum_j \beta_{ij} x_i x_j + \epsilon \quad (2)$$

Where β is the constant, m is the number of parameters, β_i is the linear coefficient, β_{ii} is the quadratic coefficient, β_{ij} is the interaction coefficient, and ϵ is the error of the parameter.

If there are three input parameters, the DOE software must input at least (12) values for each parameter to make the statistical analysis between them. Moreover, the 17 tests (runs) were made for more accurate results in this work.

The optimization process involves consolidating the combination of the many different components that have been recruited [19]. Numerical optimization plays a crucial role in the design of expert software [20].

3.3.1 Silicon Nanoparticles

Silicon nanoparticles were put through a series of tests using the DOE software per the experimental strategy. Table 2 gives the parameters specifications for silicon nanoparticles, the input parameters of laser energy, the number of pulses, and PRR, where the laser energy lower and upper values are 100 and 500 mJ, respectively. The lower and upper values of the number of laser pulses are 10 and 90, respectively. While the lower and upper PR values are 1 and 5 Hz, respectively. Moreover, the output parameters are the peak wavelength and the absorption peak. The results for Table 2 were shown in Figure 4.

Table 2 Ranges of variation in DOE input and output parameters for Nd:YAG laser with silicon

Parameter	Unit	Type	Levels		
			-1	0	1
Energy	mJ	Input	100	300	500
No. of pulses	-	Input	10	50	90
PRR	Hz	Input	1	3	5
Wavelength Peak	nm	Output	-	-	-
Absorbance Peak	-	Output	-	-	-

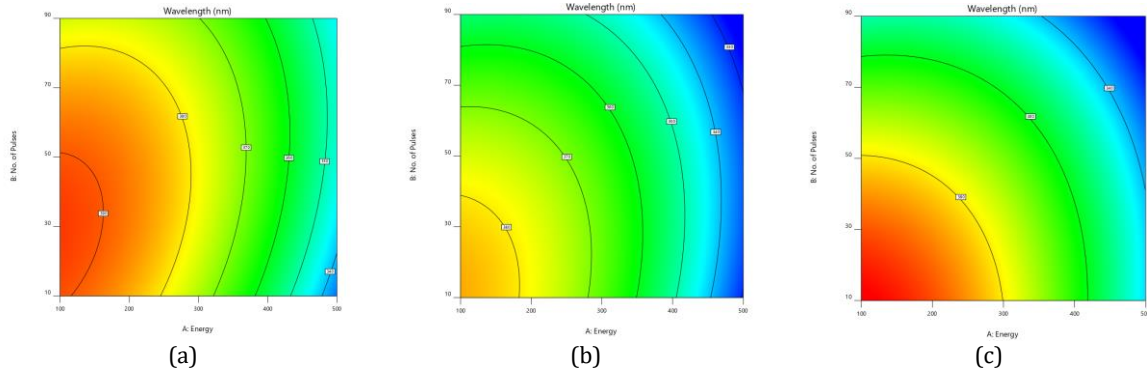


Figure 4. The 2D wavelength peak for no. of pulse and energy at PRR: (a) 1 (b) 3 (c) 5.

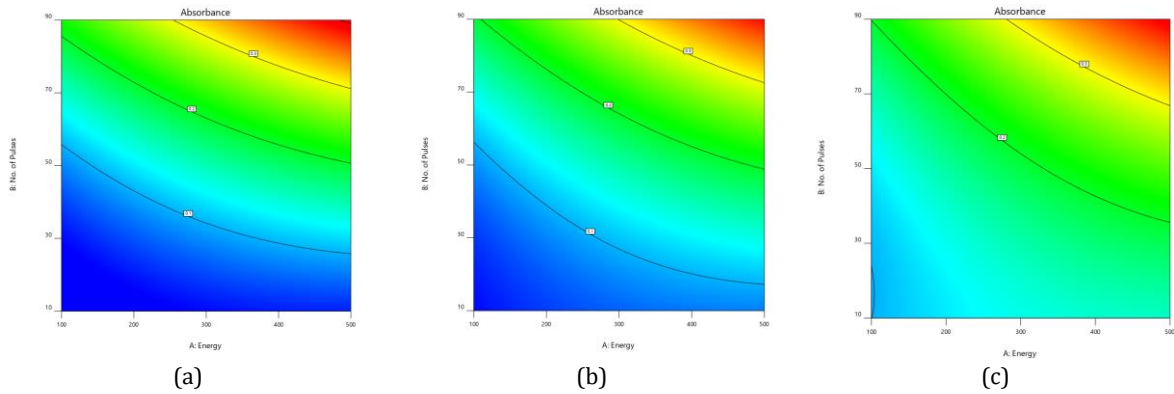


Figure 5. The 2D absorbance peak for no. of pulse and energy at PRR: (a) 1 (b) 3 (c) 5.

Figure 4 shows a contour graph of the peak wavelength at 1-5 PRR. When the laser energy was increased, the smaller silicon nanoparticles were produced. Moreover, Figure 5 shows a contour graph of the absorption peak at 1-5 PRR. When the laser pulses increase, its produced higher number of silicon nanoparticles, which leads to an

increasing the absorption of silicon nanoparticles suspension. Furthermore, when the PRR was increased, the wavelength and absorbance peaks decreased due to the smaller size of Si NPs. The optimum values of the output parameters for table 2 are shown in Figure 6.

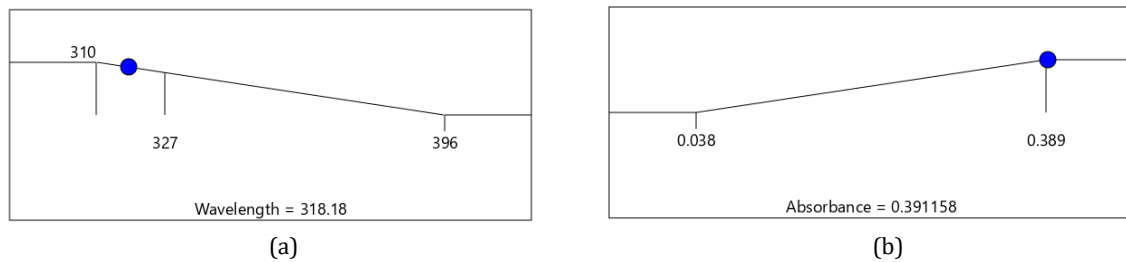


Figure 6. The Ramps solutions of optimum value for: (a) wavelength peak (b) absorbance peak.

Figure 6 shows the optimum values of the output response for silicon nanoparticles. When using Nd:YAG laser, the optimum wavelength, peak absorption values are 318.2 nm, 0.391, respectively.

3.3.2 Quartz Microprocessing

3.3.2.1 Fabrication a Microlens

Stage one was crucial in microlens fabrication because it was responsible for its initial shape and dimension. The parameters using in the Design of Expert software for the experimental strategy for stage one is presented in Table 3.

Table 3 Ranges of variation in DOE input and output parameters for fiber laser with quartz

Parameter	Unit	Type	Levels		
			-1	0	1
Power	W	Input	10	15	20
Speed	mm/s	Input	50	100	150
Count.	-	Input	1	5	9
NA	-	Output	-	-	-

Table 3 gives the parameters that used in fabrication of quartz microlens in first stage. The input parameters were laser power and laser speed and the number of repeated processes. The laser power lower and upper values are 10 and 20 W, respectively. The lower and upper values of the laser speed are 50 and 150 mm/s, respectively. While The

number of repeated processes lower and upper values are 1 and 9, respectively. Also, the numerical aperture was the output parameters. The graphical result of numerical aperture was shown in Figure 7.

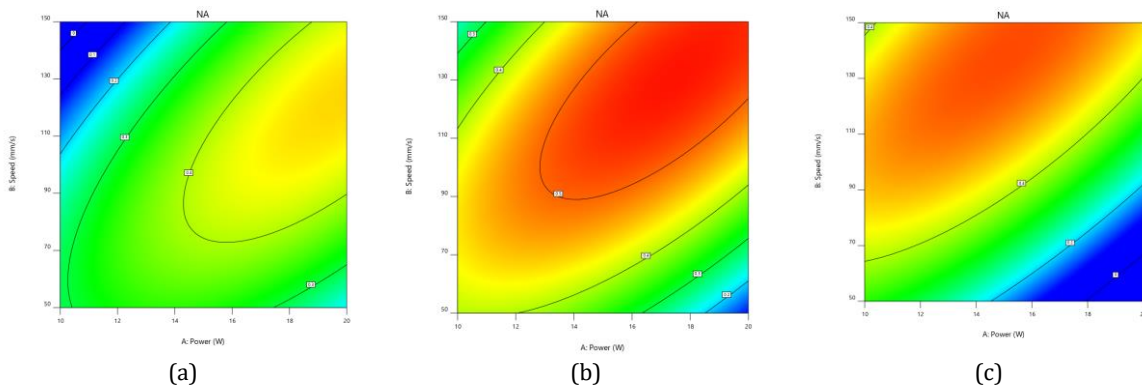


Figure 7. The 2D curve for NA, for laser power and laser speed at no. of the repeated process 1-9 times.

Figure 7 shows contour graph of the microlens NA at one to nine times repeated processes: the max. and min. At higher laser power and lower laser speed, and higher no. of repeated process, it produces deeper dip due to the high amount of ablated material and greater NA. Moreover, the NA value was increased when the repeated process was increased.

3.3.2.1 Microlens Enhancement

The reshaping stage using CO₂ laser plays a significant role in the microlens enhancement. The parameters of this stage using Design of Expert software for the experimental strategy is presented in Table 4.

Table 4 Ranges of variation in DOE input and output parameters for CO₂ laser with quartz

Parameter	Unit	Type	Levels		
			-1	0	1
Power	W	Input	3	4	5
Speed	mm/s	Input	1	3	5
Count.	-	Input	1	3	5
Roughness	nm	Output	-	-	-

Table 4 gives the experimental results of quartz microlens, the input parameters of laser power and laser speed, and the number of repeated processes. The laser power lower and upper values are 3 and 5 W, respectively.

The lower and upper values of the laser speed are 1 and 5 mm/s, respectively. The number of repeated processes for the lower and upper values is 1 and 5, respectively. Also, the lens roughness is the output parameter. The graphical result for Table 4 was shown in Figure 8.

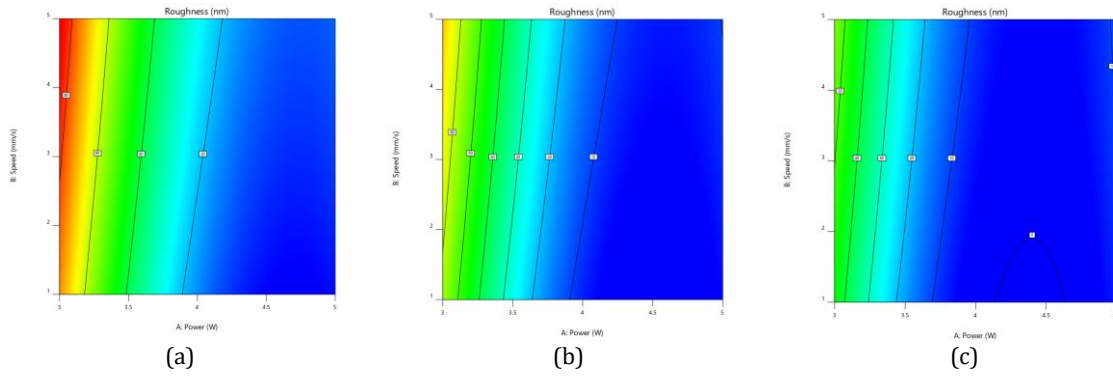


Figure 8. The roughness 2D curve for laser power and laser speed at no. of the repeated process 1-5 times.

Figure 8 shows a contour graph of the lens height at one-five times repeated processes. When the laser power was high value, laser speed was low value, and the no. of repeated process was high value, it melted the surface completely due to exceeding the melting point of the quartz material. Moreover, the roughness value was increased when the laser speed was increased. In contrast,

the roughness value was decreased when the repeated process was increased. The optimum values of the output parameters for the first and second stages are shown in Figure 9.

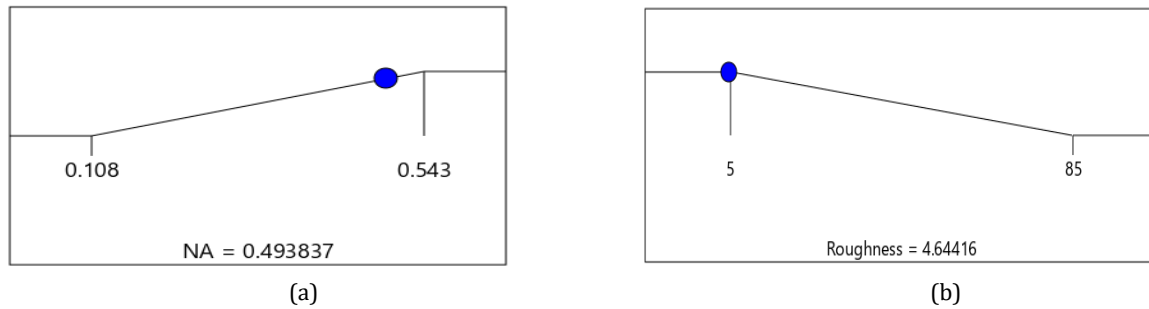


Figure 9. The Ramps solutions of optimum value for:(a) NA (b) roughness.

Figure 9 shows the optimum values of the output response for quartz microlens. the optimum NA and roughness values are 0.494 and 4.64 nm respectively.

4. CONCLUSIONS

In this study, design of expert analysis (DOE) and Box-Behnken design (BBD) software were utilized to optimize the laser microprocessing parameters for better outcomes. Theoretical calculations and COMSOL software simulations were employed to understand the surface and subsurface heat distribution in silicon and quartz during laser irradiation. Moreover, the research concludes that laser micro/nano processing, coupled with optimization techniques, offers a promising approach for fabricating silicon nanoparticles by Nd:YAG laser and quartz microlens arrays by fiber and CO₂ lasers with potential applications in various fields.

ACKNOWLEDGMENTS

This work was done at the Laser and Optoelectronics Engineering department, College of Engineering, Al-Nahrain University, Iraq, as a partial requirement of an PHD degree in laser and optoelectronics engineering.

REFERENCES

- [1] J. Wang, F. Fang, H. An, S. Wu, H. Qi, and Y. Cai, "Laser machining fundamentals: micro, nano, atomic and close-to-atomic scales," *Int. J. Extrem. Manuf. Top.*, vol. 5, pp. 1–26, 2023.
- [2] M. A. Volosova and A. A. Okunkova, "Advances in Laser Materials Processing," *Metals (Basel)*, vol. 12, no. 917, pp. 4–9, 2022.
- [3] H. Minghui, "Laser-material interaction and its applications in surface Micro Nanoprocessing," *AIP Conf. Proc.*, vol. 1278, pp. 293–302, 2010.
- [4] M. P. and V. F. U. K. Andrés Fabián Lasagni, "Fabrication and Characterization in the Micro-Nano Range," *Adv. Struct. Mater.*, vol. 10, no. 2, pp. 29–46, 2011.
- [5] L. Rihakova and H. Chmelickova, "laser micromachining of glass, silicon and ceramics. a review," *Eur. Int. J. Sci. Technol.*, vol. 4, no. 7, pp. 41–49, 2015, doi.org/10.1155/2015/584952.
- [6] M. S. Hassan, Z. A. Taha, and B. G. Rasheed, "Synthesis and Modeling of Temperature Distribution for Nanoparticles Produced Using Nd:YAG Lasers," *J. Nanotechnol.*, vol. 24, no. 5, pp. 1–8, 2016, doi: http://dx.doi.org/10.1155/2016/8560490.

- [7] R. Intartaglia, K. Bagga, M. Scotto, A. Diaspro, and F. Brandi, "Luminescent silicon nanoparticles prepared by ultra short pulsed laser ablation in liquid for imaging applications," *Opt. Mater. Express*, vol. 2, no. 5, pp. 510–518, 2012, doi: <https://doi.org/10.1364/OME.2.000510>.
- [8] W. A. Ghaly and H. T. Mohsen, "Laser-induced silicon nanocolumns by ablation technique," *J. Radiat. Res. Appl. Sci.*, vol. 13, no. 1, pp. 398–405, Jan. 2020, doi: <https://doi.org/10.1080/16878507.2020.1740395>.
- [9] C. Gaudiuso, A. Volpe, and A. Ancona, "Single-pass direct laser cutting of quartz by IR femtosecond pulses," *Proc. SPIE*, vol. 5, p. 10, 2021.
- [10] T. D. Sherpa and B. B. Pradhan, "Micro-grooving of silicon wafer by Nd:YAG laser beam machining," *IOP Conf. Ser. Mater. Sci. Eng.*, vol. 377, no. 1, pp. 1–7, 2018.
- [11] T. Schmidt and D. Conrad, "Micro lens arrays made by CO₂-laser radiation," vol. 1147806, no. July 2020, p. 39, 2020, doi: [10.1117/12.2566485](https://doi.org/10.1117/12.2566485).
- [12] A. Al-Kattan, L. M. A. Ali, M. Daurat, E. Mattana, and M. Gary-Bobo, "Biological assessment of laser-synthesized silicon nanoparticles effect in two-photon photodynamic therapy on breast cancer mcf-7 cells," *Nanomaterials*, vol. 10, no. 8, pp. 1–11, 2020, doi: [10.3390/nano10081462](https://doi.org/10.3390/nano10081462).
- [13] B. X. Wang, J. X. Zheng, J. Y. Qi, M. R. Guo, B. R. Gao, and X. Q. Liu, "Integration of Multifocal Microlens Array on Silicon Microcantilever via Femtosecond-Laser-Assisted Etching Technology," *Micromachines*, vol. 13, no. 2, 2022, doi: [10.3390/mi13020218](https://doi.org/10.3390/mi13020218).
- [14] W. R. Runyan, *Silicon Semiconductor Technology*, First edit. New York: McGraw-Hill, 1965.
- [15] P. Chewchinda, T. Tsuge, H. Funakubo, O. Odawara, and H. Wada, "Laser wavelength effect on size and morphology of silicon nanoparticles prepared by laser ablation in liquid," *Jpn. J. Appl. Phys.*, vol. 52, no. 2, pp. 1–4, Feb. 2013, doi: <https://iopscience.iop.org/article/10.7567/JJAP.52.025001>.
- [16] L. A. J. Garvie, P. Rez, J. R. Alvarez, P. R. Buseck, A. J. Craven, and R. Brydson, "Bonding in alpha-quartz (SiO₂): A view of the unoccupied states," *Am. Mineral.*, vol. 85, no. 6, pp. 732–738, 2000.
- [17] H. K. Hasan, "Analysis of the effecting parameters on laser cutting process by using response surface methodology (RSM) method," *J. Achiev. Mater. Manuf. Eng.*, vol. 110, no. 2, pp. 59–66, 2022, doi: [10.5604/01.3001.0015.7044](https://doi.org/10.5604/01.3001.0015.7044).
- [18] J. Wu, "A prediction approach of fiber laser surface treatment using ensemble of metamodels considering energy consumption and processing," *Green Manuf. Open*, vol. 3, no. 13, pp. 1–20, 2023, doi: [10.20517/gmo.2022.04](https://doi.org/10.20517/gmo.2022.04).
- [19] C. Damaris, C. Petrieanu, and G. Nagîț, "Quality Control and Optimization Of A Laser Cutting System For Cutting 10mm Mild Steel Using Doe Software," *Int. J. Mod. Manuf. Technol.*, vol. VIII, no. 1, pp. 7–11, 2016.
- [20] S. Singh, N. Yaragatti, M. Doddamani, S. Powar, and S. Zafar, "Drilling parameter optimization of cenosphere / HDPE syntactic foam using CO₂ laser Drilling parameter optimization of cenosphere / HDPE syntactic foam using CO₂ laser," *J. Manuf. Process.*, vol. 80, no. May, pp. 28–42, 2022, doi: [10.1016/j.jmapro.2022.05.040](https://doi.org/10.1016/j.jmapro.2022.05.040).
- [21] J. Ciurana and D. Teixidor, "Robotics and Computer-Integrated Manufacturing Optimization of process parameters for pulsed laser milling of micro-channels on AISI H13 tool steel," *Robot. Comput. Integr. Manuf.*, vol. 29, pp. 209–218, 2013, doi: [10.1016/j.rcim.2012.05.005](https://doi.org/10.1016/j.rcim.2012.05.005).